Volume 2, Number 1: 1-10, April 2004
Review Article

International Journal of
Vascular Biomedical Engineering

Biomedical Engineering Research on Circulatory Disorders

Jung Yul Yoo[1¶], Jae Hyung Park[2], Sangho Suh[3], Eun Bo Shim[4], Kyehan Rhee[5], Sehyun Shin[6], Young I. Cho[7], C. Sean Kim[8] and Hyung-Woon Roh[9]

[1] *School of Mechanical and Aerospace Engineering, Seoul National University*
[2] *College of Medicine, Seoul National University*
[3] *Department of Mechanical Engineering, Soongsil University*
[4] *Department of Mechanical Engineering, Kangwon National University*
[5] *Department of Mechanical Engineering, Myongji University*
[6] *School of Mechanical Engineering, Kyungpook National University*
[7] *Department of Mechanical Engineering and Mechanics, Drexel University, U.S.A.*
[8] *Central R&D Institute, Samsung Electro-Mechanics Co. Ltd*
[9] *IVAI*

Abstract

Circulatory disease is the number two cause of death next to cancer in Korea, while the cardiovascular disease alone is the number one cause of death in the US. In the present article, some background, current status and future prospects of biomedical engineering esearch on circulatory disorders are discussed in terms of the origin of atherosclerosis, computational fluid dynamics and medical imaging techniques, clinical treatments and fluid dynamics, advances in stents, hemodynamic analysis of artificial heart, and artificial blood. In particular, the importance of close collaboration of medicine and fluids engineering is emphasized.

Key words: Atherosclerosis, Computational Fluid Dynamics, Medical Imaging.

Introduction

Recently, Korea National Statistical Office reported that circulatory disorder is the number two cause of death in Korea, preceded only by cancer (Table 1).[1] And needless to say, cardiovascular disease alone is the number one cause of death in the US.[2] Circulatory disease is caused by the circulation or flow of blood, so that it is highly required to understand the characteristics of the blood and its circulation. Thus, the objective of this article is to make a general survey of the collaborations made between medicine and fluids engineering to cope with the problems encountered in circulatory diseases.

¶ San 56-1, Shinlim-dong, Kwanak-ku, Seoul, Korea
E-mail: jyyoo@snu.ac.kr

Discussion

Origin of Atherosclerosis

In the past, the causes of cardiovascular disease and arteriosclerosis were traditionally known to be hypertension and hyperlipemia. However, the fact that about half of the deaths from heart failure have normal blood pressure and cholesterol level indicated strongly that there are other causes. Atherosclerosis is a form of arteriosclerosis, and the most intriguing feature of atherosclerosis is that it is very nonuniformly distributed in the body. It occurs only at certain points on the arterial tree. In Figure 1, the prevalent locations for atherosclerosis in humans are marked by ink blots.[3] It is seen that these spots are very limited in length. Figure 2 is an angiogram and its schematic diagram of the left

coronary artery with stenosis.[4] Here, too, you can see that morbidity results from localized (focal) plaque deposition rather than from diffuse disease.

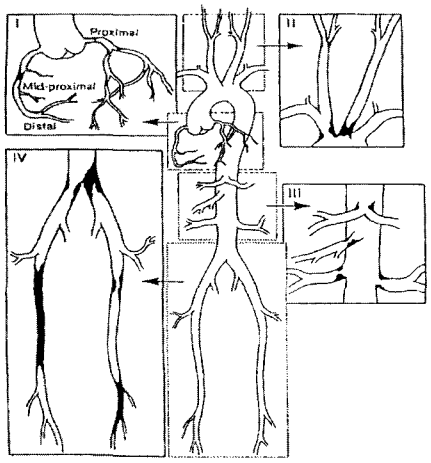

Figure 1 Distribution of atherosclerotic occlusive disease in humans.[3]

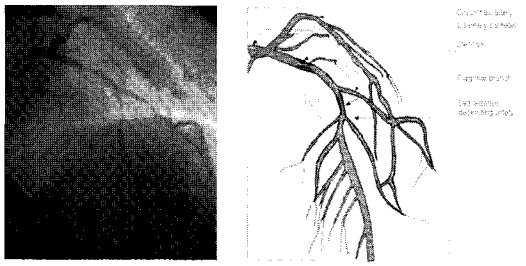

(a) angiogram (b) schematic diagram

Figure 2 Angiogram of the left coronary artery with stenosis.[4]

On the other hand, histological studies of the blood vessel found no specific markers for any protein of the blood vessel destined for atherogenesis. Fluid mechanics theorists in the 80's pointed out that the places where atherogenesis is likely to occur are places that have a relatively complex geometry, a fairly large Reynolds number, and a lower than average wall shear stress.[3] It is now widely accepted and believed in the medical world that atherosclerosis occurs at the places where the endothelium cells are deformed by the low shear, causing damages of the tunica intimae.

Figure 3 shows how atherosclerosis is generated. For high shear flow of blood, endothelial cells are aligned in the flow direction and normally deformed, so that tunica intimae are well-protected. However, for low shear flow of blood, endothelial cells tend to shrink and are rather deformed spherically, so that tunica intimae are exposed to blood and endothelial cells are further damaged, which leads to the generation of atherosclerosis.

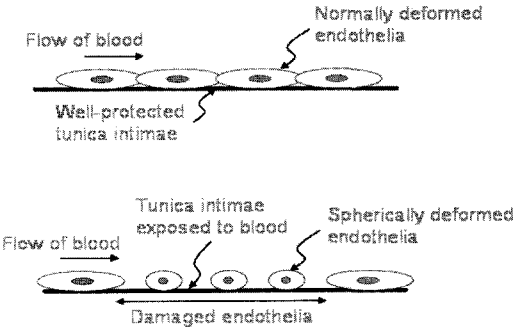

Figure 3 Atherosclerosis generation

Computational Fluid Dynamics and Medical Imaging Technique

Next discussions will be given on how CFD (Computational Fluid Dynamics) and MIT (Medical Imaging Technique) can work together to enhance our understanding of blood flow in human body, and to contribute to development of the medical art for diagnosis and treatment of circulatory disorders.

Actually this part of the present article is just an example of close collaborations between CFD and MIT, which Dr. C. S. Kim of Samsung Ltd. presented at the KSME 60th Anniversary Spring Conference.[5] Figure 4 shows an image of human cerebrovascular system.[6] There are two pairs of arteries that supply blood to human brain, i.e., a pair of carotid arteries and another pair of vertebral arteries. The left and right carotid arteries are respectively divided into ECA (External Carotid Arteries) and ICA (Internal Carotid Arteries). ECA supply the face and scalp with blood. ICA supply blood to the front 3/5 of the cerebrum, which amounts to 7.6% CO (cardiac output). Further, the left and right vertebral arteries are joined together to form a single basilar artery, supplying the back 2/5 of the cerebrum, part of the cerebellum, and the brain stem, which amounts to 4.2% CO. The left and right carotid arteries and the basilar artery are joined in the cerebrum base to form a circle which is called the Circle of Wills (CoW). According to Alpers, et al. in 1959, about 52% of the population have an "ideal" configuration.[7] However,

even though one of the main arteries is occluded, the distal smaller arteries that it supplies can receive blood from the other arteries. Therefore, the rest of the population can also live healthily unless there are other particular anomalies.

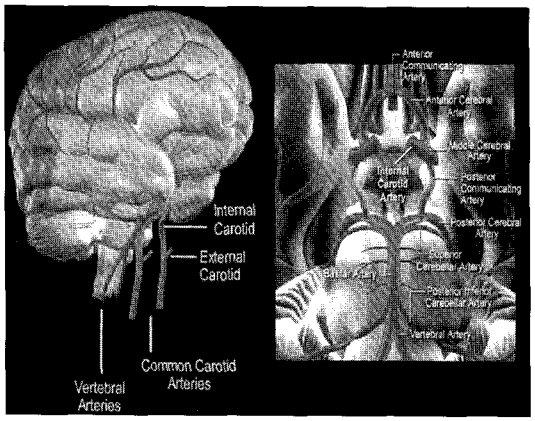

Figure 4 Latral and posteroanterior projections of human cerebrovascular system.[6]

In order to simulate the auto-regulating blood flow in a realistic configuration, an anatomical CoW model was reconstructed from subject-specific MRA images.[5] Raw MR images were converted to the RGB graphic file format for efficient numerical treatments. After extracting the segments of interest by filtering the voxels with intensities below a certain threshold, a segment outlining algorithm was used to display the extracted objects on each cross-sectional layer with very little computer memory. A commercial grid generation software Gridgen[8] was used to create a three-dimensional surface database by stacking the two-dimensional transverse outlines. A certain degree of human intervention was required for the complete connectivity between surface domains. Consequently, a multi-block grid system with 32 domains was generated for this geometry. Using this 3-dimensionally reconstructed anatomical grid system of about 2 million grid points, simulations of the auto-regulation mechanism of the cerebral arteries were carried out. Flow conditions used in the computation are as follows: left ICA diameter, D = 5.6 mm; mean velocity, U = 14 cm/s; blood density, rho = 1054 kg/m^3; blood viscosity, nu = 3.5 cPoise = 0.0035 Pa s; Reynolds number, Re = 240.0.

Figure 5 shows collateral circulation with left ICA 20% stenosed under auto-regulation. If there occurs a sudden stenosis at the left ICA by 20%, only approximately 80% of the blood flow is provided, so that those arteries which used to receive blood through this left ICA will now receive drastically reduced blood flow rates of 84.2% and 95.4%. In this case, the auto-regulation function of the brain is activated. Therefore, thanks to this auto-regulation, after 7 seconds, these two arteries are simulated to recover, respectively, 99.2% and 99.7% of their initial blood flow rates.[5] Figure 6 shows the time-dependent flow rates of the left MCA (Middle Cerebral Artery) and ACA (Anterior Cerebral Artery) after a sudden stenosis in the left ICA. It can be seen that, although the left ICA continuously provides only 80% of the normal blood flow rate, the blood flow is provided through the CoW to the left ACA and MCA. Within approximately 10 seconds, the left MCA and ACA have regained their initial (or reference) flow rates. The present numerical models combining CFD and MRI are considered to provide the patient-specific information for surgical and interventional procedures as a predictive surgery tool.[5]

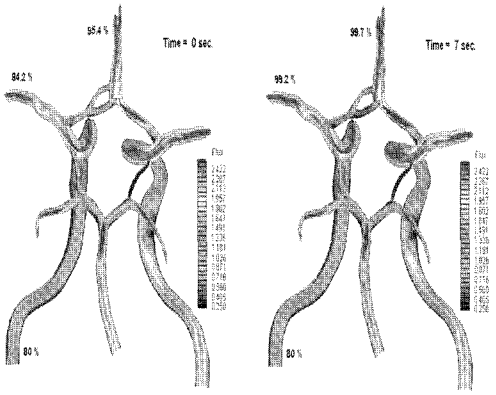

Figure 5 Collateral circulation with left ICA 20 % stenosed under auto-regulation.[5]

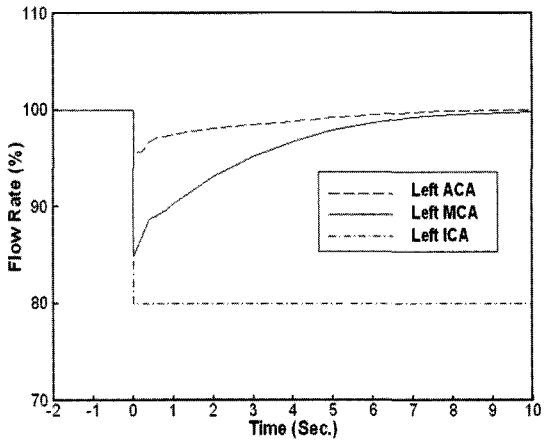

Figure 6 Percent changes of flow rate in the left middle and anterior cerebral arteries using AAR algorithm.[5]

Clinical Treatment and Fluid Dynamics

Clinical treatment of arterial disorders can be classified into intervention and bypass grafting. Intervention treatment uses stent or balloon angioplasty, and bypass grafting utilizes sequential bypass or cuff patch.

Aneurysm is a vascular disease characterized by weakening and bulging out of the portion of an artery.[9] Figure 7 shows an image of cerebral aneurysm.[10] In order to treat cerebral aneurysms, clips and coils are used to block the blood flow into the aneurysm sac. When aneurysms are partially blocked, the locations of a clip and coils influence the flow field inside the aneurysm sac which affect embolization process.[11,12,13] By using the PIV technique, the velocity fields inside the model aneurysm sacs are measured for different clip and coil locations to suggest effective surgical sites for aneurysm embolization.

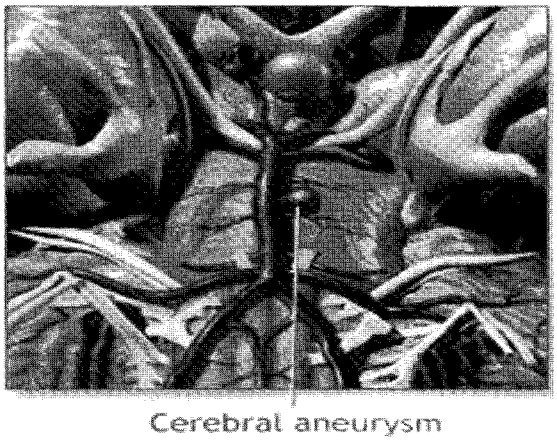

Figure 7 An image of cerebral aneurysm.[10]

Figure 8 shows the PIV data for velocity fields inside the model aneurysm sac for proximal (left figure) and distal (right figure) clip location.[11] Distally clipped aneurysm showed less flow into the aneurysm sac. Figure 9 shows the PIV data for velocity fields inside the model sac for proximal (left figure) and distal (right figure) coil location.[13] Again, distally coiled aneurysm showed less flow into the aneurysm sac. Figure 10 shows the changes of flow field, caused by stents used for fusiform aneurysm models.[14] Straight vertical marker lines are reference time lines generated by using a photochromic dye. The curved marker lines show the displacement of the reference lines within a few milliseconds. Significant reduction of the flow insides the aneurysm sac is observed by stenting.

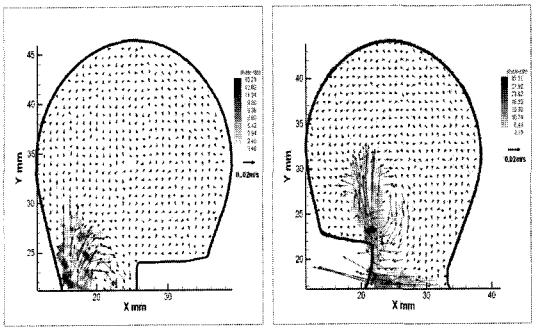

Figure 8 Aneurysm treated with a clip.[11]

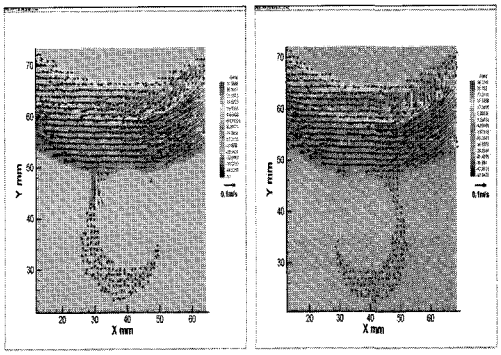

Figure 9 Aneurysm treated with coils.[12]

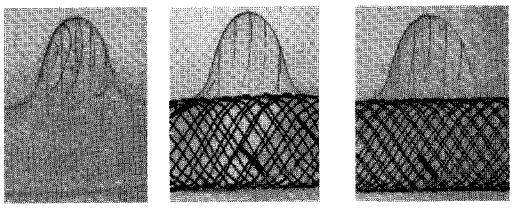

Figure 10 Aneurysm treated with a stent.[14]

In Figure 11, initial and 6-months follow-up coronary angiographies for 60 patients with angulated coronary stenosis were performed.[15] Two models were considered. Model 1 corresponds to a group of 33 patients with an angle change of less than 50%. Model 2 corresponds to a group of 27 patients with an angle change of less than 50%, so that the artery became more straight than in the case of Model 1, after stenting. 6-months follow-up coronary angiogram demonstrated that Model 2 had lower percent restenosis than Model 1, which was supported by CFD simulation results.

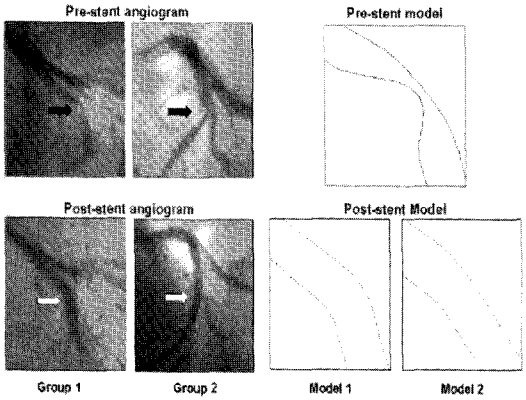

Figure 11 Coronary groups and computerized schematic models before and after stenting, based on images of the human left anterior descending artery (closed arrow: pre-stent stenosis; open arrow: post-stent). Subjects and models were grouped by percentage angle change (group and model 1, < 50%; group and model 2, > 50%).[15]

Figure 12 shows two-dimensional simulations of the velocity and pressure distributions in the stenosed coronary artery with two sequential bypasses: one uses curved blood vessel (right upper figure) and the other uses bifurcated blood vessel (right lower figure).[4] The result shows that both bypasses can smoothly supply left anterior descending artery and diagonal branch distal to the stenosis, with sufficient blood flow rate.

Figure 13 shows the results of CFD simulation for the effect of end-to-side anastomotic model with the cuff on the flow rate and impedance.[16] This study showed that the hemodynamic characteristics can be improved by inserting a cuff when the pressure difference is small, i.e., when the blood flow rate is small.

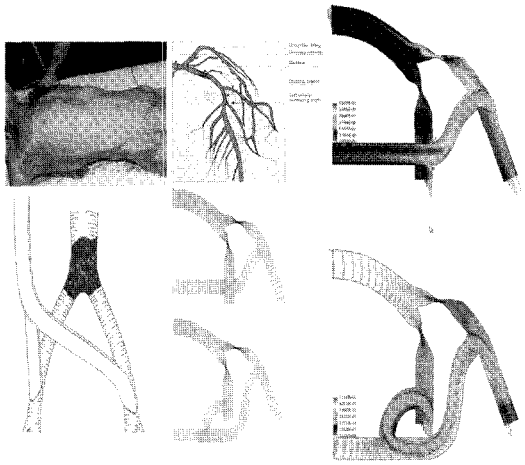

Figure 12 Extraanatomical bypass.[4]

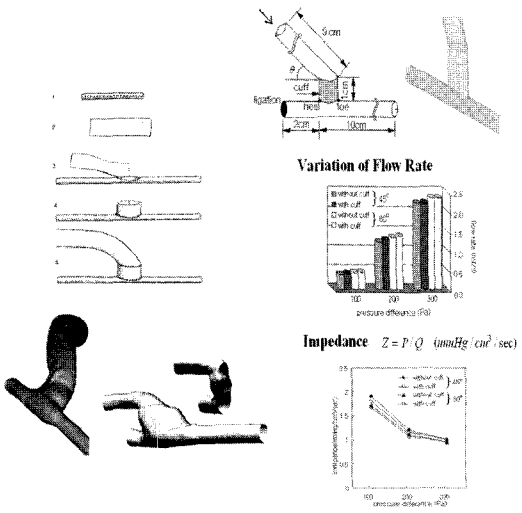

Figure 13 Cuff patch.[16]

Advances in Stents

Figure 14 shows technical evolution in vascular intervention. Since the balloon catheter was first used in 1977, it has been developed continuously to the extent that it is applied to coronary artery.[17] Very recently, stent has been developed rapidly so that even drug eluting stents are being announced. Various stents are being developed by domestic researchers. One example is the Niti-S stent developed by the research group of College of Medicine, Seoul National University, that is used for iliac artery stenosis (Fig. 15).[18,19,20]

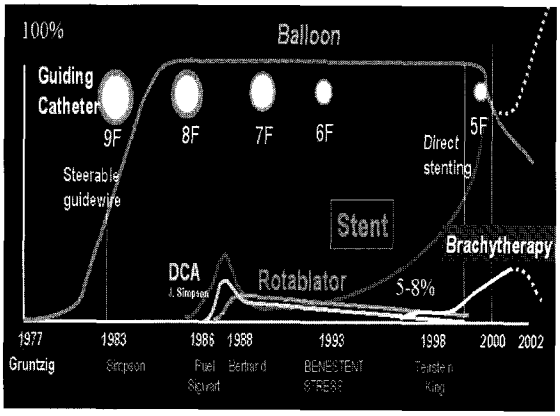

Figure 14 Technical Evolution in Vascular Intervention[17]

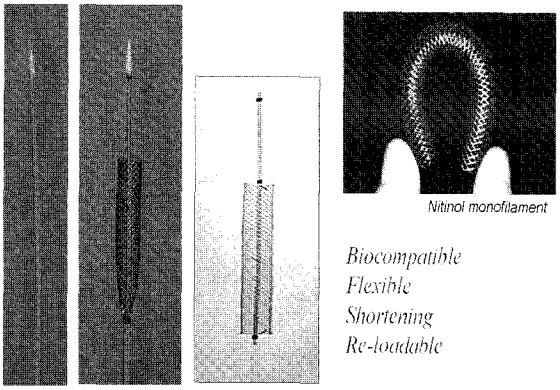

Figure 15 Self-expendable stent: Niti-S.[18,19,20]

Advances are being made towards ideal metallic stent meeting various requirements:[17]

* Easy deployment
* Flexible in tortuosity
* Low profile
* No migration
* High expansion ratio
* Thromboresistant
* Variable size, length
* Thin neointima
* Radiopacity
* Iso-compliant
* Precise targeting
* Biologically inert
* Retrievable
* Less fatigue
* High hoop strength
* Imaging application
* Resist to deformation
* Inexpensive

Physical characteristics and structure of a stent have a significant effect on the stent performance and hemodynamic improvement. Figure 16 shows design and cell geometry of ballooning stents. For aneurysm, a stent-graft can be used which is a combination of metallic stent and vascular graft.[21,22] The most excellent one known so far is the stent made by Zenith Cook Company, which is expected to replace many of the surgical operations of the aneurysm.[23] Figure 17 shows an example of the treatment of a patient with abdominal aorta aneurysm by inserting a stent-graft.[24]

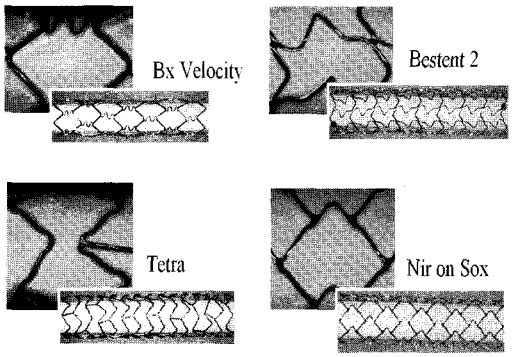

Figure 16 Stent design and cell geometry.[21,22]

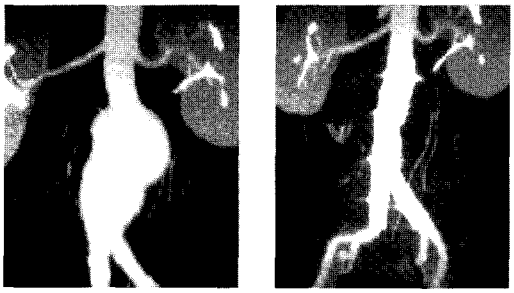

Figure 17 Stent-graft for AAA.[24]

Hemodynamic Analysis of Artificial Heart

Artificial hearts can be classified into 5 types. LVAD (Left Ventricular Assist Device) is used for temporary applications with post-cardiotomy patients. BiIVAD (Biventricular Assist Device) functions as a right ventricle as well as a left ventricle. BiVAD with atrial cannulation lasts 3 – 6 months, and is used as a bridge to recovery. BiVAD with ventricular cannulation lasts 6 – 12 months and is applicable to ventriculectomy patients. THA (Total Artificial Heart) is used for permanent replacement.

ECLS (Extracorporeal Life Supporting System) is used for emergency patients suffering from respiratory arrest.

Since 1985 Korean Artificial Heart has been developed by Prof. Byung Goo Min at Seoul National University.[25,26] In 2000, a cactus-type artificial heart named AnyHeart was developed, which can be used for TAH, LVAD, and BiVAD. In 2001, haman transplantation of artificial heart was carried out by Prof. Kyung Sun at Korea University, which was the first clinical application of AbioCor Implantable Replacement Heart which is a product of ABIOMED, USA.[27] In the same year, a pulsatile ECLS was invented, based on the principle of Korean Artificial Heart, which is being applied to animal experiment and theoretical study.[25,26]

Figure 18 shows the cactus-type artificial heart which was named Anyheart because it can serve various purposes, as LVAD, BiVAD, TAH, ECLS, etc. Figure 19 is a schematic for hemodynamic analysis of AnyHeart. Left figure shows how AnyHeart is connected with the cardiovascular system, and right figure shows two blood sacs and actuators installed inside the artificial heart. At the inlet and exit of the blood sacs there are jellyfish-type artificial heart valve prostheses. This valve operates like an umbrella: when the umbrella is opened, the valve is closed, and vice versa. The movement of the mechanism starts as the actuator pushes alternately the left and right blood sacs by an oscillating motion. Accordingly, the blood flow inside the sac is formed.

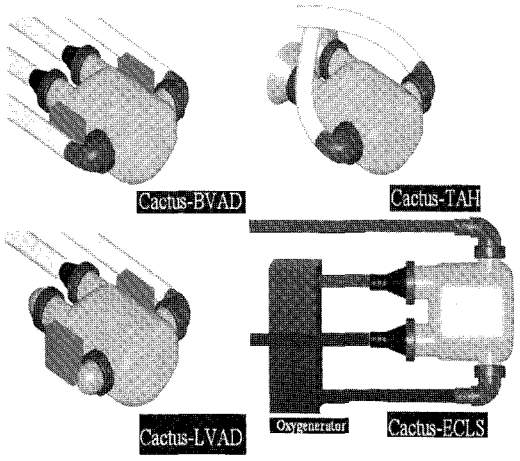

Figure 18 Cactus-type artificial heart named AnyHeart[25]

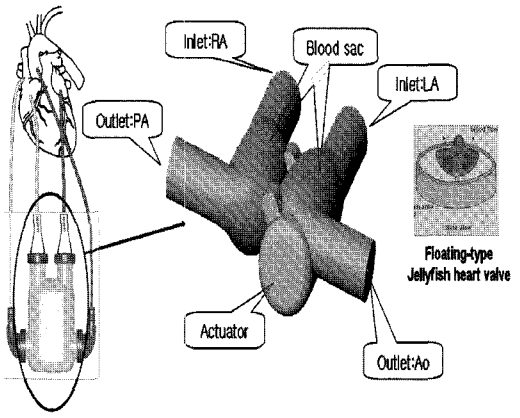

Figure 19 Schematic of AnyHeart.[25]

To analyze this, we have to consider collectively the fluid motion inside the blood sac, the solid mechanics of the sac material, and the contact problem between the actuator and the sac material. However, for simplicity we consider three-dimensional solid (sac) – fluid (blood) interaction, by assuming that the blood is an incompressible viscous fluid and the sac is a linearly elastic isotropic solid. The deformation of the blood sac by the actuator is replaced with time-varying pressure boundary condition at the blood sac surface. That is, the deformation is induced by imposing the pressure distribution on the blood sac surface, which is observed experimentally to cause the actual deformation. Consequently, this deformation will be the driving force to generate the internal blood flow. Figure 20 shows the surface grids used in the present analysis. On the left is the grid for undeformed shape, and on the right is the grid for maximally deformed shape.

In the present study, ADINA is adopted, which is a commercial S/W based on finite element method.[28] Among the numerical result obtained for one cardiac cycle (approximately 1 sec), Figure 21 shows instantaneous velocity distributions at a point of time during the filling phase and at another point of time during the ejection phase. On the left, the velocity distributions at various cross sections show very well that the blood is being filled with the inlet valve open and the outlet valve closed during the filling phase. The right figure shows that during the ejection phase the blood is being ejected with the outlet valve open and the inlet

valve closed. Near the inlet valve, a stagnation region is being formed and near the exit valve the fluid with strong gradient is being ejected. Figure 22 shows the shear stress distribution duirng the ejection phase indicating a strong

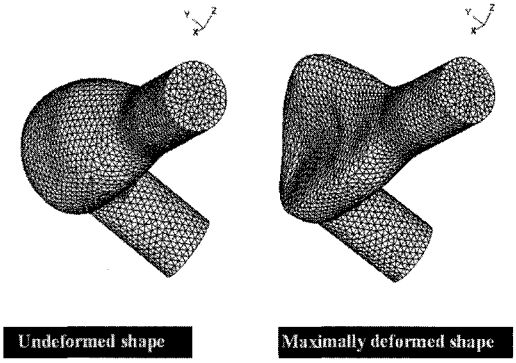

Figure 20 Surface grids used in the numerical analysis of 3-dimensional blood flow in the Korean Artificial Heart.[26]

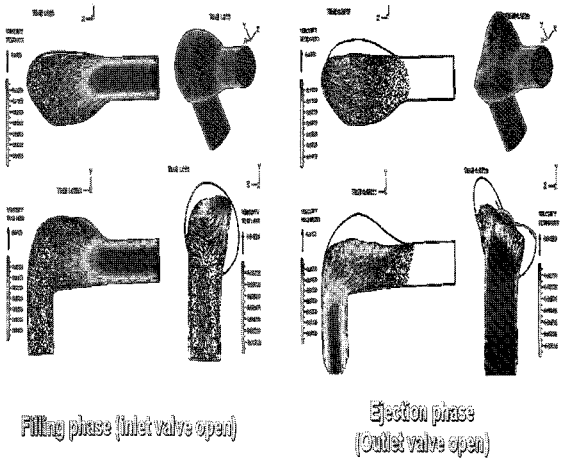

Figure 21 Instantaneous velocity distribution during the filling and ejection phases.[26]

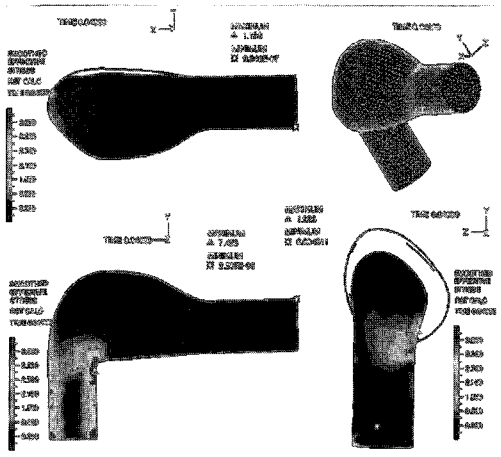

Figure 22 Shear stress distributions during the ejection phase.[26]

gradient at the wall in the exit region. The maximum value occurs at the innermost corner which looks like a wedge in the lower left figure. Thus, the ultimate goal of such computer simulation is to realize the most optimal shape of the artificial heart on which the most appropriate stress distribution is applied, by utilizing the computational result for minimum and maximum stresses.

Artificial Blood

Artificial blood is an intravascular oxygen carrier (blood substitute) which is designed to temporarily augment oxygen delivery in patients and is applicable to the patient at risk of acute tissue oxygen deficit due to either transient anemia, blood loss, or ischemia. Development of a hemoglobin-based blood substitute was pursued vigorously by the military throughout the Vietnam War. Oxygen carrying capability of perfluorocarbons (PFC) is approximately 100 times greater than that of plasma. Development of emulsifying agents which are stable and bio-compatible is under way. PFC is a biologically inert solution and is safe for intravenous infusion. PFC has been developed by utilizing new emulsifying agents such as perflubron (perfluorooctyl bromide). A commercial PFC emulsion Oxygent^{TM} is being developed by Alliance Pharmaceutical Corp.[29]

A series of experiment was performed where survival in a rat model of lethal hemorrhagic shock is prolonged following resuscitation with a small volume of a solution containing a DRP (drag-reducing polymer) derived from aloe vera.[30] The test rats are divided into 3 groups. DRP group is treated by resuscitating with DRP of less than 10 ppm (parts per million). NS group is treated by resuscitating with normal saline (NS). Control group received no resuscitation. As Shown in Figure 23 resuscitation with DRP prolongs survival in rats with lethal hemorrhagic shock. Figure 24 shows that DRP reduces the thickness of cell-free layer near the blood vessel, even though the adding amount is only about several ppm. Several DRP candidates are under examination. The requirements for new DRP are that they

must be compatible with all blood types and have no effect on aggregability and deformability of blood cells.

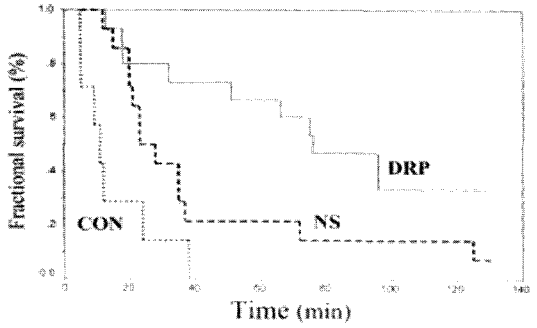

Figure 23 Fractional survival rate in a rat model of lethal hemorrhagic shock.[30]

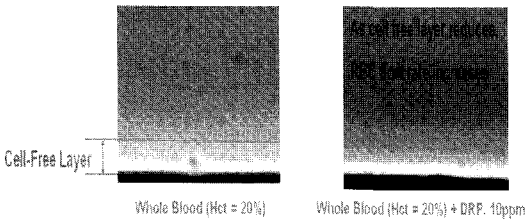

Figure 24 Cell-free layer near the blood vessel.

Conclusion

It has been discussed how fluid mechanics theory has contributed to identification of the places where circulatory disorders occur and how the CFD techniques can contribute to diagnosis and treatment of circulatory disorders. Biomedical engineering research in which researchers in the fields of medicine, biology, chemistry, physics, materials, electronics as well as mechanical engineering work together can cover a wider scope of circulatory disorders by making more active interactions.

Acknowledgements

The corresponding author would like to extend his deepest thanks to Prof. Kyung Sun of Korea Artificial Organ Center for inviting him to "International Symposium on Artificial Organs: Present and Future," on the occasion of 100th Anniversary of Korea University, where he could present a large portion of this article.

References

1. http://www.nso.go.kr.
2. http://www.truestarhealth.com.
3. Fung YC. Biomechanics: Circulation, Springer-Verlag New York Inc. 1997.
4. Roh HW, Suh SH, Kwon HM, Lee BK. Sequential bypass effects in the stenosed coronary artery. Proceedings of the KSME 2003 Spring Conference (CD ROM). 2003;1919-1922.
5. Kim CS. Computational simulation of auto-regulatory brain circulation using CFD and MRA techniques, Proceedings of the KSME 2005 (60th Anniversary) Spring Conference (CD ROM). 2005;2702-2707.
6. http://www.strokecenter.org.
7. Alpers BJ, Berry RG, Paddison RM. Anatomical studies of the circle of Willis in normal brain," Arch. Neurol. Psychiatry. 1959;81:409-418.
8. http://www.pointwise.com.
9. Mayberg MR, Batjer HH, Darcey R. Guidelines for the management of aneurysmal subarachnoid hemorrhage. Circulation 1994;90:2592-2605.
10. http://www.adam.com.
11. Lin T, Fox AJ, Drake CG. Regrowth of aneurysm sacs from residual neck following clipping. J Neurosurgery 1989;70:556-560.
12. Graves VB, Strother CM, Partington CR, Rappe A. Flow dynamics of lateral carotid artery aneurysms and their effects on coils and balloons: An experimental study in dogs. AJNR 1992;13:189-196.
13. Gobin YP, Counord JL, Flaud P, Duffaux J. In vitro study of hemodynamics in a giant saccular aneurysm model: influence of flow dynamics in the parent vessel and effects of coil embolisation. Neuroradiology 1994;36:530-536.
14. Wotton DM, Ku DN. Fluid mechanics of vascular systems, diseases, and thrombosis. Ann Rev Biomed Eng 1999;299-329.
15. Lee BK, Lee J, Hong BK, Park BE, Kim D, Kim DY, Cho YH, Yoon SJ, Yoon YW, Kwon HM, Roh HW, Kim I, Park HW, Han SM, Cho MT, Suh SH, Kim HS. Hemodynamic analysis of coronary

circulation in angulated coronary stenosis following stenting. Yonsei Medical Journal 2002;43:5:590-600.

16. Suh SH, Roh HW, Yoo SS. Investigation on hemodynamic characteristics for the end-to-side anastomosis with cuff. '98 Workshop on Biomedical Fluid Dynamics 1998;7-16.
17. Becker GJ. Vascular Stent: Abram's Angiography. 1997.
18. Lee KW, Park JH, Chung JW, Kim WS, Lee W, Yeon KM. Short-term effects of a new intravascular nitinol stent in canine arteries. Invest Radiol 1999;34:367-373.
19. Yoon CJ, Chung JW, Park JH, Hong SH, Song SY, Lim HG, Lee YS. A newly designed nitinol stent: early clinical experience in the treatment of iliac artery stenoses and occlusions. Korean J Radiol 2001;2:145-150.
20. Yoon CJ, Chung JW, Kim HB, Lee JW, Park JH. A new nitinol monofilament stent: early experience with use for transjugular intrahepatic portosystemis shunts. Cardiovasc Intervent Radiol 2002;25:200-204.
21. Park JH, Chung JW, Joh JH, Song SY, Shin SJ, Chung KS, Lee DY, Won JY, Kim SJ. Aortic and arterial aneurysm in Behcet's disease: management with stent-grafts-initial experience. Radiology 2001;220:745-750.
22. Chuter TA. The choice of stent-graft for endovascular repair of abdominal aortic aneurysm. J Cardiovasc Surg (Torino) 2003;44:519-525.
23. http://www.zenithstentgraft.com.
24. Ohki T, Veith FJ, Shaw P, et al. Increasing I ncidence of midterm and long-term complications after endovascular graft repair of abdominal aortic aneurysms: a note of caution based on a 9-year experience. Ann Surg 2001;234:323-335.
25. Shim EB, Yeo JY, Ko HJ, Youn CH, Lee YR, Park CY, Min BG, Sun K. Numerical analysis of the three-dimensional blood flow in the Korean artificial heart. Artificial Organs 2003;27:1:49–60.
26. Jeong GS, Shim EB, Ko HJ, Youn CH, Sun K, Min BG. Computational analysis of the three-dimensional hemodynamics of the blood sac in the twin-pulse life-support system. J Artif Organs 2004;7:174–180.
27. http://www.abiomed.com.
28. www.adina.com.
29. http://www.alp.com.
30. Carlos AM, Kameneva MV, Tenhunen JJ, Puyana JC, Fink MP. Survival in a rat model of lethal hemorrhagic shock is prolonged following resuscitation with a small volume of a solution containing a drag-reducing polymer derived from aloe vera. Shock 2004;22:2:151-156.